Estimation of the decay rate of ^{7}Be and $^7Be_2$ encapsulated in C_{70}

A. V. Bibikov,[1] A. V. Nikolaev,[1,2] and E. V. Tkalya[3,4,5,*]

[1]*Skobeltsyn Institute of Nuclear Physics, Lomonosov Moscow State University, Leninskie gory, Moscow, RU-119991, Russia*

[2]*Moscow Institute of Physics and Technology, RU-141700 Dolgoprudny, Russia*

[3]*P. N. Lebedev Physical Institute of the Russian Academy of Sciences, 119991, 53 Leninskiy pr., Moscow, Russia*

[4]*National Research Nuclear University MEPhI, Kashirskoe shosse 31, Moscow RU-115409, Russia*

[5]*Nuclear Safety Institute of RAS, Bol'shaya Tulskaya 52, Moscow RU-115191, Russia*

(Received 24 April 2019; published 6 December 2019)

Electron capture (β-decay) rates of ^{7}Be and $^7Be_2$ encapsulated in C_{70} have been estimated by calculating the electron density $\rho(0)$ at the ^{7}Be nucleus and comparing it with $\rho(0)$ and experimental β-decay rates of ^{7}Be inside another fullerene—C_{60}. For that the endohedral fullerenes ^{7}Be@C_{70} and $^7Be_2$@C_{70} have been examined by means of the *ab initio* approach using the Hartree-Fock method with the the second order Møller-Plesset perturbation theory accounting for the Van der Waals foces. Our calculations indicate that the $^7Be_2$@C_{70} complex is stable with the binding energy of 1.3 eV and the ^{7}Be dimer bond length 2.30 Å. It has been found that $\rho(0)$ is practically the same in ^{7}Be@C_{70} and $^7Be_2$@C_{70}, but larger than in an isolated ^{7}Be atom. The increase of $\rho(0)$ however is smaller than in ^{7}Be@C_{60}. We also discuss in detail the mechanism underlying the increase of $\rho(0)$ and consequently the decrease of the decay rate in ^{7}Be@C_{70} in comparison with the isolated ^{7}Be atom.

DOI: 10.1103/PhysRevC.100.064603

I. INTRODUCTION

Measurements of the electron capture (or K capture) by the ^{7}Be nucleus is a well-known method to study chemical bonding and the influence of chemical environment on atomic electron shells of beryllium [1,2]. The $(1s)^2(2s)^2$ electron shell of the Be atom is a very suitable choice for such research. That is because (1) the wave function amplitude of s states has its largest value at the nucleus, (2) the contribution from the $2s$ valence states of Be to the total electron density at nucleus, $\rho(0)$, is relatively large and amounts to 3.2%, and (3) the $2s$ electrons of Be participate in chemical bonding which affects the probability of the ^{7}Be nuclear decay.

First measurements of the ^{7}Be nuclear decay constant demonstrating its dependence on the chemical state of the ^{7}Be atom have been performed in the middle of the last century in Refs. [1–7]. Today, dozens of studies (reviewed in Ref. [8]) on half-lives $T_{1/2}$ and decay constants $\lambda = \ln(2)/T_{1/2}$ for the ^{7}Be nucleus in various chemical environments are available. On average, deviations of $T_{1/2}$ and λ for ^{7}Be implanted in Cu, Al, Au, Al_2O_3, Pd, W, LiF, or participated in chemical compounds ^{7}BeO, $^7BeO_2$, $^7BeF_2$, $^7BeBr_2$, etc. (see Ref. [8]) lie within 1%.

The first decade of 21st century is marked by the start of the research on the endohedral fullerene ^{7}Be@C_{60} [9–12]. It has been established experimentally that the ^{7}Be half-life in the ^{7}Be@C_{60} molecule is appreciably decreased in comparison with the benchmark decay in metallic beryllium, and it is in fact the fastest decay of ^{7}Be among all observed. Following experimental works theoretical models developed in [8,12–14] described the data for ^{7}Be@C_{60} not only qualitatively, but also quantitatively, and even predicted an inverse effect—a considerable increase of the ^{7}Be half-life in the molecule ^{7}Be@C_{36} [8].

Endohedral fullerene complexes A@C_{60} are also useful for studying other types of radioactive decay. Of particular importance is the decay of the low lying isomeric state of the ^{229}Th nucleus in fullerenes. This decay proceeds through the channel of internal conversion, that is, through the $(6d)^2(7s)^2$ valence electron states of Th [15,16]. It is worth noting that these electron shells of Th are most affected by its interaction with the fullerene cage. Therefore, it is conceivable that this mechanism can also lead to a substantial change of the decay rate of the isomeric state of ^{229}Th.

Two theoretical methods have been applied to the study of the ^{7}Be@C_{60} endohedral fullerene—the density functional approach (DFT) [9,12] and the Hartree-Fock (HF) method [13]. The DFT method takes into account correlation effects, but needs a special treatment to take into account the weak dispersive forces. The Hartree-Fock method with the second order perturbation correction (HF+MP2) captures weak Van der Waals molecular forces between ^{7}Be and the fullerene cage. In order to assess the electron density at the ^{7}Be nucleus one uses numerical basis functions (DMol^3) or a special set of narrow Gaussian s-basis functions [13]. Nevertheless, both methods lead to the same qualitative conclusions concerning the comparative study of the electron density at the ^{7}Be nucleus in ^{7}Be@C_{60}, the ^{7}Be metal and the isolated ^{7}Be atom, albeit the numerical values are slightly different. These discrepancies are very small lying within the numerical error associated with the method used. A thorough comparison between the numerical values of $\rho(0)$ in both approaches is given in the work [13].

*tkalya_e@lebedev.ru

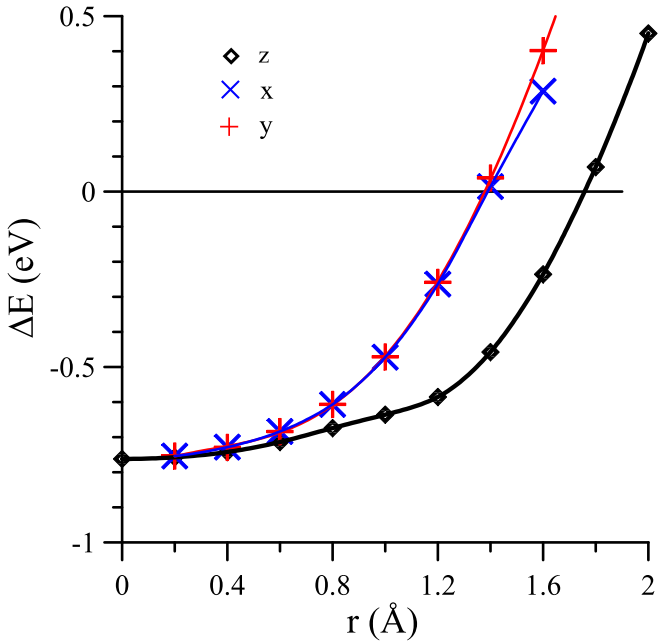

FIG. 1. HF+MP2 energy of ^{7}Be@C_{70} as a function of the displacement of the ^{7}Be atom from the center of the C_{70} fullerene. Energies for displacements along x and y axes practically coincide at $r < 1.4$ Å, but become noticeably different at larger r, when the ^{7}Be atom is closer to the fullerene cage with different arrangement of neighboring C atoms.

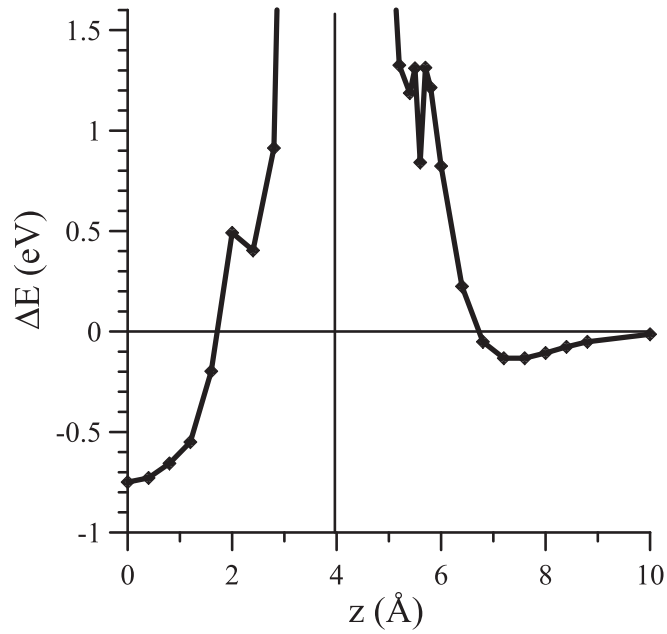

FIG. 2. The ground-state energy of the ^{7}Be@C_{70} complex as a function of the position of ^{7}Be along the z axis (HF+MP2 calculation). The black vertical line at approximately 4 Å stands for the outermost pentagon C-ring of C_{70}.

In this paper we present a new work concerning the influence of endohedral fullerenes on the electron capture of the ^{7}Be nucleus in the molecular complexes ^{7}Be@C_{70} and $^7Be_2$@C_{70}. It is organized as follows. In Sec. II we investigate the ^{7}Be@C_{70} molecule. Here we find the optimal position of the ^{7}Be atom (Sec. II A), calculate the electron density at the ^{7}Be nucleus (Sec. II B), and discuss in detail the mechanism of the increase of $\rho(0)$ (Sec. II C). Next, we consider the $^7Be_2$ dimer encapsulated in C_{70}, Sec. III. Our conclusions are summarized in Sec. IV.

II. SINGLE ^{7}Be ATOM INSIDE THE C_{70} FULLERENE

In comparison with the highly symmetric C_{60} molecule with the icosahedral group I_h, the symmetry of the C_{70} fullerene is low (D_{5h}). The main symmetry operation is the fivefold rotational axis, with five symmetry independent C atoms giving rise to eight inequivalent C–C bond lengths, ranging from 1.38 to 1.48 Å [17]. The C_{70} cage can be viewed as composed of two halves of the C_{60} fullerene fused with a belt of ten C atoms in its equatorial plane. We consider the C_{70} molecule in its standard orientation with respect to a rectangular coordinate system. The molecule is centered at the origin, its fivefold axis is taken as the z axis, the (x, y) plane is a mirror plane.

A. Optimal positions of ^{7}Be in respect to the C_{70} fullerene

We have carried out *ab initio* quantum-mechanical Hartree-Fock calculations [18,19] of the ^{7}Be@C_{70} energy using the 6–31G** molecular basis set [20]. In addition, the weak Van der Waals forces between the ^{7}Be atom and the fullerene cage, constituting dispersion forces correlations have been included by taking into account the second order correction to the total energy within the Møller-Plesset perturbation theory (MP2) [21].

First, we displace the ^{7}Be atom from the molecular center in all directions and calculate the change of the energy of the molecular complex. The results are shown in Fig. 1. We conclude that the displacement of the ^{7}Be atom away from the z axis is unfavorable leading to a steep energy rise.

After that we have studied the (HF+MP2) energy dependence along the z axis, Fig. 2. As before, we have found that the displacement in the (x, y) plane is unfavorable. In fact the energy dependencies for these directions look very similar to that for C_{60}, because the distances from ^{7}Be to nearest neighboring C atoms are as in ^{7}Be@C_{60}.

From Fig. 2 we infer that there are four minima for the ^{7}Be atom. The first global minimum is at -0.76 eV when ^{7}Be is located inside C_{70} at its molecular center. The second minimum at -0.13 eV corresponds to the ^{7}Be atom situated outside the molecule at the distance of 3.3 Å from fullerene outermost pentagon facet. The ^{7}Be atom there is bound to the fullerene cage by the Van der Waals force. Finally, two local minima are found at the distance of 1.7 Å on both sides of the fullerene facet. In the following we shall not consider them because their binding energy is ≈1 eV higher.

B. Electron density $\rho(0)$ at the ^{7}Be nucleus

Next, we calculate the electron density $\rho(0)$ at the beryllium nucleus when the ^{7}Be atom is located at the global

TABLE I. Calculated electron density (in a.u.$^{-3}$) at ^{7}Be nucleus in various environment.

	Orbitals			
	1s(Be)	2s(Be)	Others	Total
^{7}Be@C_{60}	34.221	1.245	0.021	35.487
^{7}Be@C_{70}	34.226	1.193	0.024	35.443
^{7}Be atom	34.252	1.137	–	35.389

minimum at the fullerene center. For that we have used an enlarged cc-pVTZ basis set developed earlier in [8]. In this method the cc-pVTZ basis set employed for accurate electron density calculations has been supplemented by a set of narrow s-functions $f_i = \exp(-\lambda_i r^2/2)$ with λ_i ranging from 0.1 to 10^8 a.u.$^{-2}$ (a.u. here stands for the atomic unit of length). These additional basis functions are required to achieve a converged value for the electron density at the ^{7}Be nucleus.

The results of these calculations together with the data for ^{7}Be@C_{60} and the isolated ^{7}Be atom are given in Table I. Note that the electron density at ^{7}Be inside C_{70} is increased in comparison with the value of $\rho(0)$ for an isolated atom, that is $\triangle\rho(0) > 0$, but the effect is less pronounced than in the case of ^{7}Be@C_{60}. From Table I we find that the amount of the increase for ^{7}Be@C_{70} is 55% of the effect for ^{7}Be@C_{60}. As for ^{7}Be@C_{60} the main contribution to $\triangle\rho(0)$ is due to the yield of the 2s orbital, 0.056 a.u.$^{-3}$. The contribution to $\triangle\rho(0)$ from the 1s orbital is negative, -0.026 a.u.$^{-3}$, but it is almost fully compensated by the effect from the other molecular orbitals which are delocalized on the fullerene cage.

C. Mechanism of the increase of $\rho(0)$ in ^{7}Be@C_{70}

Qualitatively the increase of the 2s electron density of ^{7}Be at its nucleus can be understood as follows. The 2s-atomic orbital of the ^{7}Be atom has a single node at 0.59 a.u. When ^{7}Be is inside the C_{70} molecule, the 2s orbital acquires additional minima at radii 5.7 and 7.8 a.u. due to the presence of the attractive potential of the fullerene nuclei, Fig. 3. These minima in fact correspond to two nodes of the 2s wave function of ^{7}Be, but the node at 5.7 a.u. slightly suppressed by a small admixture of C_{60} molecular orbitals. The 2s electron density around these additional minima is decreased, but the integral of the density keeps unchanged. Therefore, there must be a small increase of the 2s electron density in the region 0–5 a.u., and in particular around the ^{7}Be nucleus. For the first time this mechanism was put forward in [13] for the explanation of the effect for the increase of $\rho(0)$ at the ^{7}Be nucleus in the ^{7}Be@C_{60} complex. In ^{7}Be@C_{60} additional minima are found at 5 and 7 a.u. [13], situated around the C_{60} radius (6.7 a.u.). In ^{7}Be@C_{70} the fullerene shape is elongated with carbon nuclei located at radii ranging from 6.7 to 7.9 a.u. As a result, the effective attraction is distributed smoothly in the same range and additional 2s minima are situated at 5.7 and 7.8 a.u., Fig. 3. In comparison with the C_{60} fullerene, these nodes are shifted to larger radii. Since at larger radii the 2s wave function is noticeably smaller, this effect becomes less pronounced in comparison with ^{7}Be@C_{60} [13].

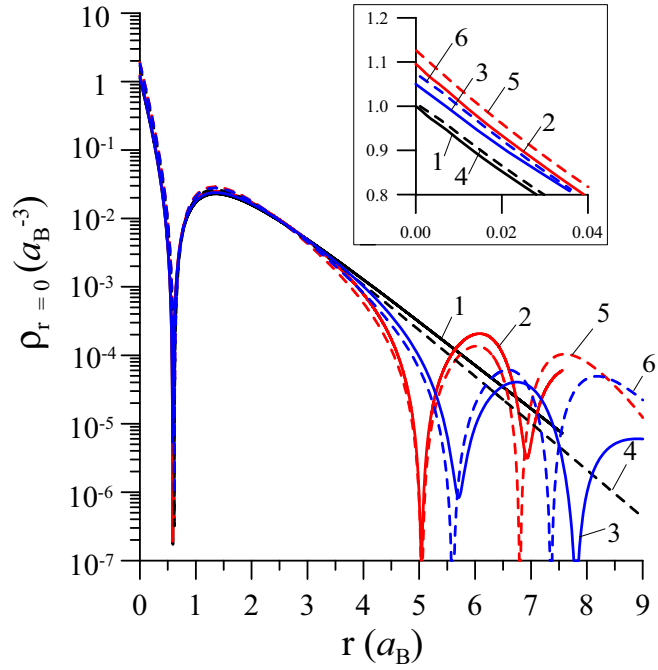

FIG. 3. The electron density $\rho_{2s}(r)$ of the 2s orbital of ^{7}Be in various environment. Isolated ^{7}Be atom: (1) HF, (4) model (see below); ^{7}Be@C_{60}: (2) HF, (5) model; ^{7}Be@C_{70}: (3) HF, (6) model. Here, "HF" stands for HF+MP2 *ab initio* calculations, while "model" for calculations with the model attractive potential simulating the attractive potential of the fullerene cage, see text for details. Inset: $\rho_{2s}(r)/\rho_{2s}^{\rm Be}(0)$ at the vicinity of the ^{7}Be nucleus. $\rho_{2s}^{\rm Be}(0)$ is the 2s density of the isolated ^{7}Be atom.

This scenario has been fully supported by our model calculations with a spherically symmetrical potential of the gaussian shape placed at an effective radius $R_{\rm eff}$ from the ^{7}Be atom, Fig. 3. Earlier, this potential has been tested for the ^{7}Be@C_{60} endohedral fullerene [13]. The depth of the potential is $U_0 = 3$ Hartree and width $w = 1$ a.u. For the effective radius of the potential we took an average value of the distances between the carbon atoms of C_{70} and the beryllium atom, $R_{\rm eff} = 7.25$ a.u. The results are presented in Fig. 3, where for comparison we also reproduce plots for the isolated ^{7}Be atom and ^{7}Be@C_{60}. The model attractive potential leads to the appearance of two nodes on both sides of $R_{\rm eff}$ and the increase of the 2s electron density at small radii $R \approx 0$ as shown in the inset of Fig. 3.

On the basis of our *ab initio* (HF+MP2) calculations supported by the model considerations we conclude that the total electron density $\rho(0)$ at the ^{7}Be inside the C_{70} fullerene becomes 0.16% larger and the half-life of the decay 0.16% smaller than $\rho(0)$ and $T_{1/2}$ for the isolated ^{7}Be atom.

III. TWO ^{7}Be ATOMS INSIDE THE C_{70} FULLERENE

In this section we discuss two beryllium atoms put inside the same fullerene cage. This situation is encountered in some experiments and practical applications involving fullerene molecules.

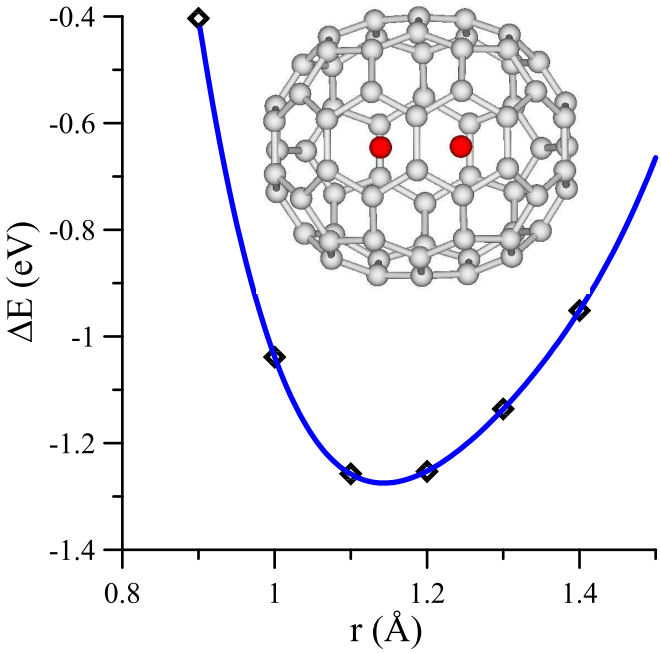

FIG. 4. Calculated (HF+MP2) energy change of the $^7Be_2@C_{70}$ complex, $\triangle E = E(^7Be_2@C_{70}) - E(C_{70}) - 2E(^7Be)$, as a function of z. Two Be atoms are located at z and $-z$ ($x = y = 0$). The binding energy is $E_b = -\triangle E$.

Our estimations for the C_{60} molecule show that placing two ^{7}Be atoms inside this fullerene is energetically unfavorable, resulting in a large increase of the total energy and a positive binding energy for the whole complex. The increase of the total energy however is smaller than the potential barrier of the fullerene cage. On the other hand, the fullerene complex is much more stable when only one ^{7}Be atom is inside C_{60} while the other ^{7}Be atom being outside is bound to the C_{60} cage by the Van der Waals force.

The situation is very different for the C_{70} fullerene. Having larger internal volume, it can easily accommodate two ^{7}Be atoms inside. As for a single ^{7}Be atom, we have found that the displacement along the x and y directions is unfavorable. For a fixed distance $d_{\text{Be-Be}}$ between two ^{7}Be atoms, the minimum of energy corresponds to a symmetrical arrangement of ^{7}Be atoms: first at z, second at $-z$ ($z = d_{\text{Be-Be}}/2$). We then computed the energy change, $\triangle E = E(^7Be_2@C_{70}) = E(C_{70}) - 2E(^7Be)$, as a function of z. The results are shown in Fig. 4 (HF+MP2 calculations with the 6–31G** basis set). From Fig. 4 we obtain that the binding energy of $^7Be_2@C_{70}$ is ≈1.3 eV with the ^{7}Be–^{7}Be equilibrium bond length $d_{\text{Be-Be}} = 2.30$ Å. This value is 0.15 Å shorter than the experimentally found bond length (2.45 Å) of the beryllium dimer [22]. Apparently, the action of the C_{70} fullerene on the $^7Be_2$ molecule is equivalent to the external pressure effect.

Finally, we have performed the calculation of electron density $\rho(0)$ at ^{7}Be nuclei following the procedure described in detail in the previous section. The result is $\rho(0) = 35.439\,\text{a.u.}^{-3}$ for $^7Be_2@C_{70}$ (for $^7Be@C_{70}$ we had $\rho(0) = 35.443\,\text{a.u.}^{-3}$). Thus within the accuracy of the calculations we have found that $\rho(0)$ for the $^7Be_2@C_{70}$ molecule coincides with the value for a single ^{7}Be nucleus inside the C_{70} fullerene given in Table I. Therefore, the decay half-life will be approximately the same as for $^7Be@C_{70}$.

IV. CONCLUSIONS

Summarizing, we have considered the molecular systems $^7Be@C_{70}$ and $^7Be_2@C_{70}$, where in the framework of the *ab initio* Hartree-Fock approach with the MP2 correction accounting for the Van der Waals forces, we have carried out accurate estimations of the electron density at ^{7}Be nuclei and the relative probability of their β decay, Table I.

Within the accuracy of our calculations, the electron density and the probability of the electron capture by ^{7}Be in the endohedral complexes $^7Be_2@C_{70}$ and $^7Be@C_{70}$ coincide. Similarly to $^7Be@C_{60}$, we have found an increase of the electron density at the ^{7}Be nucleus in $^7Be_2@C_{70}$, but the effect amounts to only 55% of that for $^7Be@C_{60}$. We have thoroughly discussed the mechanism of the increase of $\rho(0)$ performing a set of calculations with a model potential, Sec. II C. Qualitatively, the effective can be explained by the appearance of additional nodes of the $2s$ wave function of Be, which slightly pushes the electron density away from the fullerene cage and thereby increases it around the nuclear region. The effect is less pronounced for C_{70} since its effective size is larger. In the case of $^7Be@C_{36}$ the situation changes drastically [8]. All ^{7}Be–C distances in $^7Be@C_{36}$ are relatively short and the C_{36} fullerene potential pulls the electron density from ^{7}Be to its cage, causing a strong "oxidation" effect and effectively reducing the value of $\rho(0)$ at the ^{7}Be nucleus.

Since the half-life $T_{1/2}$ (or the decay constant $\lambda = \ln 2/T_{1/2}$) is usually measured experimentally, we can use our results to predict the lifetime of the ^{7}Be nucleus. Modern computer *ab initio* codes allow us to calculate the electron shell of atoms with high accuracy. Therefore, a comparison of theoretical and experimental data on the decay of the ^{7}Be nucleus in an isolated atom could serve as an ideal basis for such a recount. In the absence of such experimental data we present in Table II the electron densities and the corresponding half-lives of ^{7}Be based on the most accurate

TABLE II. The estimated ^{7}Be nucleus half-life in various environment.

Molecular System	$T_{1/2}$, days	Electron density, a.u.$^{-3}$
$^7Be@C_{60}$	52.47	35.487
$^7Be@C_{70}$	52.54	35.443
$^7Be_2@C_{70}$	52.54	35.439
^{7}Be (atom)	52.62	35.389
^{7}BeO	53.52	34.791
^{7}Be (metal)	53.55	34.770
$^7Be@C_{36}$	53.90	34.544
$^7Be^{2+}$	54.19	34.360

experimental data on the half-lives of ^{7}Be in C_{60} at low temperature [11].

Note that all obtained results can be tested experimentally, since the differences in the ^{7}Be decay are accessible at the present level of experimental accuracy [9–11].

As a corollary of the calculations, we have predicted the stability of the $^7Be_2@C_{70}$ complex with the effective binding energy of ≈1.3 eV.

ACKNOWLEDGMENTS

The authors are grateful to Prof. V. I. Kukulin for drawing our attention to the importance of the calculation of $^7Be_2@C_{70}$. This research was supported by a grant of the Russian Science Foundation (Project No. 19-72-30014). It was carried out using the equipment of the shared research facilities of HPC computing resources at Lomonosov Moscow State University [23].

[1] E. Segre, Phys. Rev. **71**, 274 (1947).
[2] R. Daudel, Revue Scientifique **85**, 162 (1947).
[3] E. Segre and C. E. Wiegand, Phys. Rev. **75**, 39 (1949).
[4] R. F. Leininger, E. Segre, and C. Wiegand, Phys. Rev. **76**, 897 (1949).
[5] E. Segre and C. Wiegand, Phys. Rev. **81**, 284 (1951).
[6] R. F. Leininger, E. Segre, and C. Wiegand, Phys. Rev. **81**, 280 (1951).
[7] J. J. Kraushaar, E. D. Wilson, and K. T. Bainbridge, Phys. Rev. **90**, 610 (1953).
[8] E. V. Tkalya, A. V. Avdeenkov, A. V. Bibikov, I. V. Bodrenko, and A. V. Nikolaev, Phys. Rev. C **86**, 014608 (2012).
[9] T. Ohtsuki, H. Yuki, M. Muto, J. Kasagi, and K. Ohno, Phys. Rev. Lett. **93**, 112501 (2004).
[10] A. Ray, P. Das, S. K. Saha, S. K. Das, J. J. Das, N. Madhavan, S. Nath, P. Sugathan, P. V. M. Rao, and A. Jhingan, Phys. Rev. C **73**, 034323 (2006).
[11] T. Ohtsuki, K. Ohno, T. Morisato, T. Mitsugashira, K. Hirose, H. Yuki, and J. Kasagi, Phys. Rev. Lett. **98**, 252501 (2007).
[12] T. Morisato, K. Ohno, T. Ohtsuki, K. Hirose, M. Sluiter, and Y. Kawazoe, Phys. Rev. B **78**, 125416 (2008).
[13] E. V. Tkalya, A. V. Bibikov, and I. V. Bodrenko, Phys. Rev. C **81**, 024610 (2010).
[14] A. V. Bibikov, A. V. Avdeenkov, I. V. Bodrenko, A. V. Nikolaev, and E. V. Tkalya, Phys. Rev. C **88**, 034608 (2013).
[15] V. F. Strizhov and E. V. Tkalya, Zh. Eksp. Teor. Fiz. **99**, 697 (1991) [Sov. Phys. JETP **72**, 387 (1991)].
[16] E. V. Tkalya, Phys.-Usp. **46**, 315 (2003).
[17] A. V. Nikolaev, T. J. S. Dennis, K. Prassides, and A. K. Soper, Chem. Phys. Lett. **223**, 143 (1994).
[18] T. H. Dunning, Jr., J. Chem. Phys. **90**, 1007 (1989).
[19] A. Artemyev, A. Bibikov, V. Zayets, and I. Bodrenko, J. Chem. Phys. **123**, 024103 (2005).
[20] M. M. Francl, W. J. Pietro, W. J. Hehre, J. S. Binkley, M. S. Gordon, D. J. DeFrees, and J. A. Pople, J. Chem. Phys. **77**, 3654 (1982).
[21] A. Szabo and N. S. Ostlund, *Modern Quantum Chemistry* (McGraw-Hill, Dover, 1989).
[22] V. E. Bondybey, Science **227**, 125 (1985).
[23] V. Sadovnichy, A. Tikhonravov, Vl. Voevodin, and V. Opanasenko, *"Lomonosov": Supercomputing at Moscow State University* in *Contemporary High Performance Computing: From Petascale Toward Exascale* (Chapman & Hall/CRC Computational Science, Boca Raton, USA, 2013), p. 283.